INFECTION AND IMMUNITY, May 2009, p. 2000–2009 Vol. 77, No. 5
0019-9567/09/$08.00+0 doi:10.1128/IAI.01070-08

Involvement of SOCS3 in Regulation of CD11c$^+$ Dendritic Cell-Derived Osteoclastogenesis and Severe Alveolar Bone Loss$^\nabla$

Xiaoxia Zhang,[1] Mawadda Alnaeeli,[1,3] Bhagirath Singh,[2] and Yen-Tung A. Teng[1,3]*

Laboratory of Molecular Microbial Immunity, Division of Periodontology, The Eastman Department of Dentistry, and Department of Microbiology and Immunology, School of Medicine and Dentistry, University of Rochester, Rochester, New York 14620[1]; Department of Microbiology and Immunology, Schulich School of Medicine and Dentistry, The University of Western Ontario, London, Ontario N6A 5C1, Canada[2]; and Center for Osteoimmunology and Biotechnology Research, College of Dental Medicine, Kaohsiung Medical University and University Hospital, Kaohsiung, Taiwan[3]

Received 27 August 2008/Returned for modification 16 October 2008/Accepted 20 February 2009

To investigate the role of suppressor of cytokine signaling (SOCS) molecules in periodontal immunity and RANKL-mediated dendritic cell (DC)-associated osteoclastogenesis, we analyzed SOCS expression profiles in CD4$^+$ T cells and the effect of SOCS3 expression in CD11c$^+$ DCs during periodontal inflammation-induced osteoclastogenesis and bone loss in nonobese diabetic (NOD) versus humanized NOD/SCID mice. Our results of ex vivo and in vitro analyses showed that (i) there is significantly higher SOCS3 expression associated with RANKL$^+$ T-cell-mediated bone loss in correlation with increased CD11c$^+$ DC-mediated osteoclastogenesis; (ii) the transfection of CD11c$^+$ DC using an adenoviral vector carrying a dominant negative SOCS3 gene significantly abrogates TRAP and bone-resorptive activity; and (iii) inflammation-induced TRAP expression, bone resorption, and SOCS3 activity are not associated with any detectable change in the expression levels of TRAF6 and mitogen-activated protein kinase signaling adaptors (i.e., Erk, Jnk, p38, and Akt) in RANKL$^+$ T cells. We conclude that SOCS3 plays a critical role in modulating cytokine signaling involved in RANKL-mediated DC-derived osteoclastogenesis during immune interactions with T cells and diabetes-associated severe inflammation-induced alveolar bone loss. Therefore, the development of SOCS3 inhibitors may have therapeutic potential as the target to halt inflammation-induced bone loss under pathological conditions in vivo.

Inflammatory bone diseases affect a large portion of the skeletal system, particularly those portions underlying mucosal surfaces, where inflammation-induced bone loss is closely associated with elevated osteoclast (OC) activity (15, 48). Inflammation-induced bone loss is readily manifested in periodontal disease (i.e., periodontitis), resulting in attachments loss, including periodontal connective tissues and supporting alveolar bone, as a consequence of the interplays between the specific subgingival biofilm and the host's immune/inflammatory responses (36, 37). The tumor necrosis factor (TNF) family member receptor activator of NF-κB ligand (RANKL), its receptor, RANK, and the natural antagonist, osteoprotegrin (OPG), have been shown to be the key regulators of the differentiation, activation, and survival of OCs and OC. precursors (5, 16–18, 23–25, 44, 55, 58). In addition, it is now clear that the host responses, especially T-cell immunity, play a pivotal role in regulating osteoclastogenesis and homeostasis of the bone tissues (termed osteoimmunology [5]). Activated CD4$^+$ T cells express RANKL, which can directly trigger osteoclastogenesis and bone loss, and they can also negatively regulate RANKL activity via OPG production. For instance, it has been shown that OPG treatment results in significantly reduced bone loss in arthritis, osteoporosis, and cancer-related bone metastasis (16–18, 24, 45, 48, 55, 58). In murine models of periodontitis, OPG injections yield a robust inhibition of alveolar bone loss of up to 80 to 100%, suggesting that the RANKL-RANK/OPG axis is the key pathway controlling periodontal osteoclastogenesis (6, 27, 46, 49, 53). In addition to its importance in regulating bone remodelling, RANKL-RANK signaling is also critical for lymph node formation and organogenesis and is involved with dendritic cell (DC) survival and DC–T-cell interactions (23, 55, 59) in which modulation of a complex cytokine network in osteoclastogenesis in vivo has been suggested and shown (45, 52, 53).

DCs are efficient antigen-presenting cells (APCs) necessary for regulating T-cell immunity (9). They are detected in diseased tissues of periodontitis and arthritic joints, where they form aggregates with T-cell infiltrates in the inflammatory foci (9, 40, 53) and are believed to contribute indirectly to inflammation-induced bone loss. Recent studies showed that Flt3$^+$ monocyte/macrophage (Mo/MQ) precursors may differentiate to OCs, microglia, or DCs, thereby suggesting that these cell types may share common progenitors (2, 9, 26, 32). We recently reported the development of functional OCs from a CD11c$^+$ DC subset(s) capable of inducing bone resorption in vitro and post-adoptive transfer in vivo (called DC-derived OCs [DDOC]) (1–4). Moreover, under arthritic conditions, human Mo-derived DCs have been shown to *trans*-differentiate into OCs in vitro, collectively suggesting that DCs may contribute directly to pathological bone loss (1, 2, 38). Thus,

* Corresponding author. Mailing address: The Eastman Dental Center, University of Rochester Medical Center, Box 683, 625 Elmwood Ave., Rochester, NY 14620. Phone: (585) 275-7309. Fax: (585) 473-5254. E-mail: andy_teng@urmc.rochester.edu.

$^\nabla$ Published ahead of print on 2 March 2009.

further understanding of the molecular mechanisms during DC–T-cell interactions driving disease pathogenesis and the resulting bone loss is imperative to facilitate the development of novel therapeutics for future treatments.

Suppressors of cytokine signaling (SOCS) family and cytokine-inducible SH2 domain-containing protein (CIS) are cytoplasmic adaptor proteins that regulate various cytokine responses in leukocytes via negative feedback loops to inhibit inflammatory stimuli (62). There are eight members, including SOCS 1 to 7 and CIS, and each contains an N terminus, a central SH2 domain, and a C-terminal SOCS box. SOCS inhibits cytokine signaling by binding to phosphorylated JAKs and cytokine receptors and interacting with E3 ubiquitin ligases to polyubiquitylate JAKs for degradation (62). Several studies have investigated the roles of SOCS family members in regulating the development and function of immune cells. For instance, SOCS1 and -3 contain a kinase inhibitory region (KIR) in the N terminus, which inhibits JAK tyrosine kinase activity (35, 60, 61). As cytokine signaling activates JAK/STAT pathways, yielding activated SOCS molecules, SOCS1 is known to bind to JAKs with inhibitory catalytic activity and SOCS3 binds to its proximal sites on cytokine receptors, thereby directly inhibiting JAK signaling (62). These studies established the involvement of SOCS1 and SOCS3 molecules in regulating APCs (i.e., DCs) and T-cell functions during both innate and adaptive immunity (61, 62). Meanwhile, researchers have just begun to elucidate the effects of SOCS expression on the development of OCs and OC precursors, whereby specific SOCS molecules regulating osteoclastogenesis via cytokine signaling have been shown (35, 62). To date, however, the role(s) of SOCS family molecules and their impact on modulating RANKL expression and alveolar bone destruction in periodontal lesions remain unclear. Of particular interest to us is SOCS3, as it has been previously shown to be involved during inflammation-induced osteoclastogenesis and its activity is closely associated with key osteotropic cytokines, such as interleukin-1 (IL-1), TNF-α, transforming growth factor β, IL-6, IL-17, etc. (8, 10, 11, 35, 43, 60).

We and others have established the NOD and humanized NOD/SCID mouse models to study periodontal inflammation and immunity and discovered that diabetic NOD mice manifest enhanced alveolar bone loss associated with increases in (i) T-cell proliferation and RANKL expression postinfection by anaerobic *Aggregatibactor actinomycetemcomitans* compared to prediabetic and nondiabetic NOD mice, and (ii) the Th1-inducing capability of the $CD11c^+$ DC subset (14, 27–29). The enhanced alveolar bone loss in diabetic NOD and the physiological relevance of humanized NOD/SCID to periodontitis (14, 27, 49, 63) provide robust systems to study disease pathogenesis during the host-microbe interactions and alveolar bone loss. Herein, we employed these established animal models to assess the role of key SOCS molecules during periodontal immunity and RANKL-mediated alveolar bone loss by studying SOCS expression profiles in pathogen-reactive $CD4^+$ T cells and the impact of halting functional SOCS3 on the development and activity of $CD11c^+$ DDOC.

MATERIALS AND METHODS

Mice, study subjects, cell cultures, and reagents. In the present study, there were a total of 89 NOD/SCID, 200 NOD/LtJ (*H-2*^{g7} [*K*^{d} *A*a^d *Ab*^{g7} *E*^{null} *D*^{b}]), 30 NOR, and 60 BALB/c (*H-2*^{d}) mice, all of which were females, 8 to 9 weeks of age, obtained from our breeding suites of the animal colony at the Eastman Dental Center, University of Rochester, or purchased from The Jackson Laboratory (Bar Harbor, ME) and housed in a specific-pathogen-free unit. All NOD mice were monitored for type 1 diabetes by daily measurement of their urine ketone and glucose levels by using Diastix strips and blood glucose by using a Glucometer Elite XL meter (Bayer, Toronto, Canada). Keto-Diastix strips (Bayer) were used for daily monitoring and diagnosis. Mice were considered diabetic when whole-blood glucose levels exceeded 200 mg/dl on two to three consecutive days, with the histological evidence of severe lymphocytic infiltration in the pancreatic β-islets (insulitis) where 70 to 80% female NOD mice developed diabetes by age 16 to 20 wks. Diabetic mice were treated for hyperglycemia with humulin U insulin (1 to 4 units/day; Eli Lilly, Indianapolis, IN) to maintain urine ketones (0 to 0.5 unit) and glucose at <2 units on the Keto-Diastix strips. All NOD mice were categorized based on their age and the state of diabetes as follows: mice 6 to 8 weeks that were considered prediabetic with periinsulitis, mice >12 to 16 weeks old with blood glucose levels of <140 mg/dl that did not develop diabetes and were considered nondiabetic, and mice >16 to 20 weeks old with blood glucose levels of >200 mg/dl and insulitis that were considered diabetic as reported previously (27, 28).

To establish human peripheral blood leukocytes (HuPBL)-engrafted NOD/SCID mice, four aggressive periodontitis patients (AgP1 to -4; mean age, 21 ± 4.4 years) and three age-matched disease-free healthy subjects were recruited as described previously (27, 49, 54, 63). The experimental protocol has been previously described (27, 54, 63). Briefly, on day 1, 25×10^6 to 30×10^6 freshly prepared mononuclear leukocytes from HuPBL samples (AgP1 to -4) via centrifugation with Percoll were injected intraperitoneally into the NOD/SCID mice (10 to 16 mice/blood donor) after sublethal irradiation with ≤250 rads (49). This was repeated once per week for the first 2 to 3 weeks and the levels of individual HuPBL engraftment into the NOD/SCID mice established were comparable to those reported in our previous studies (≥30%) (49, 54, 63). Informed consent was obtained from all participants and all experimental protocols were approved by the human ethics and animal experimentation committees of the University of Rochester.

All primary cell cultures were performed in complete RPMI 1640 medium supplemented with 10% heat-inactivated fetal bovine serum (Invitrogen Life Technologies), 50 μM 2-mercaptoethanol, 100 μg/ml streptomycin, and 100 U/ml penicillin. Cells were incubated at 37°C in a humidified 5% CO_2 incubator. The following reagents were purchased from commercial sources: recombinant murine granulocyte-macrophage colony-stimulating factor (mGM-CSF; Cedarlane Laboratories); anti-mFcRIII/II (CD16/32), phosphatidylethanolamine (PE)-conjugated anti-mCD4, fluorescein isothiocyanate (FITC)-conjugated anti-mCD11c, peridinin chlorophyll protein (PerCP) Cy5.5-conjugated anti-mCD4, rat anti-mI-A^d, biotin anti-mCD31 (ER-MP12), biotin anti-mLy-6C (ER-MP20), rat anti-murine T-cell receptor (mTCR)/αβ-chain, rat anti-mCD3, recombinant murine IL-4 (rmIL-4), and concanavalin A (ConA) (BD Pharmingen); FITC-conjugated goat anti-hFc-γ (The Jackson Laboratory); magnetic bead-conjugated anti-mCD11c (Miltenyi Biotec); anti-mM-CSF (R&D Systems); recombinant human gamma interferon (rhIFN-γ), anti-mFc-R (CD16/32), anti-mCD4, PE-conjugated anti-h/m CD4, FITC- or allophycocyanin-conjugated goat anti-hFc-γ and anti-h/m IL-4, PE- or PerCP-Cy5.5-conjugated anti-h/mIFN-γ (BD Pharmingen, Toronto, Canada); goat anti-rabbit biotinylated immunoglobulin G (IgG), and streptavidin-PE molecules (Vector Lab, CA); and rmRANKL and OPG-Fc fusion proteins were prepared as described previously (1, 14, 27, 49, 54).

$CD11c^+$ DC^+ T-cell and *A. actinomycetemcomitans* cocultures, TRAP, and bone resorption assays for in vitro osteoclastogenesis. $CD11c^+$ DCs were generated from bone marrow (BM) of BALB/c, NOD, and NOR mice using a previously described protocol (1). Briefly, total BM cells freshly isolated from long bones were cultured with 20 ng/ml rmGM-CSF and 10 ng/ml rmIL-4 to generate DCs. On day 7, $CD11c^+$ DCs were purified by using magnetic bead-conjugated mCD11c monoclonal antibodies (MAb) and a magnetic-activated cell sorting (MACS) device (Miltenyi Biotec). The resulting population is highly pure (>98%) (1). To generate $mCD4^+$ T cells, total splenocytes were prepared from syngeneic NOD, NOR, or BALB/c mice after lysis of red blood cells. Splenocytes were passed through a nylon-wool column to enrich T cells, after which $CD4^+$ T cells were further purified via direct panning on an anti-mCD4-GK1.5 MAb-coated petri dish. The yielded $CD4^+$ T cells were 95 to 97% pure (1). Purified 0.5×10^6 $CD11c^+$ DCs were cocultured with $CD4^+$ T cells (1:1 to 1:5 ratio) on hydroxyapatite (HA)-coated 48-well plates in triplicates with or without the following reagents: *A. actinomycetemcomitans* sonicate antigens (Ags; 10 μg/ml), ConA (5 μg/ml), or rmRANKL (30 ng/ml). DC cocultures were incubated for 4 to 5 days, during which DCs were assessed for TRAP and resorptive pits (lacunae) activities, as well as surface phenotype by flow cytometry and immunoflu-

orescence microscopy as described below. DC viability was assessed by trypan blue exclusion during the coculture period. Splenocytes (0.5×10^6) stimulated by ConA for 3 to 4 days were used as the positive control.

In parallel, 0.5×10^6 to 1×10^6 purified *A. actinomycetemcomitans*-reactive periodontal $CD4^+$ T cells derived in vitro as reported previously (14, 27, 49, 54) were harvested and subjected to immunostaining for their cell surface expression of RANKL (OPG-Fc-FITC or allophycocyanin labeled) and intracellular staining after being fixed by 4% formaldehyde and permeabilized with 0.2% Triton X-100 followed by incubation with IgG conjugate for the expression of IFN-γ (PE coupled or PerCP-Cy5.5, a True-Red fluorochrome conjugate for flow cytometry analysis with excitation at 490 and 675 nm and emission at 695 nm) and IL-4 (FITC coupled) by fluorescence-activated cell sorting (FACS) analysis described previously. For FACS scanning, cells were gated on live lymphocytes and analyzed for RANKL expression in $CD4^+$ T cells using FACSCalibur and CellQuest software (BD Biosciences).

$CD11c^+$-DC cocultures were fixed with 2% formaldehyde plus 0.2% glutaraldehyde in phosphate-buffered saline (PBS; pH 7.3) for 45 min. Then, cells were incubated with TRAP staining solution (0.2 sodium acetate buffer, 40 mM sodium tartrate, 1.2 mM naphthol AS-MX phosphate, and 1.3 mM Fast Red violet Luria-Bertani salt). To quantify TRAP signals (1), images were captured digitally under 400× magnification using a Leica inverted IRBE-DM microscope via a motorized staging facility equipped with a high-resolution Hamamatsu-Orca digital camera. Both total numbers and total surface area of (purple-red) $TRAP^+$ multinucleated cells (more than or equal to three nuclei) were quantified as described previously (1). Briefly, 15 to 17 randomly chosen fields (covering 33 mm^2, or one-third of the total surface areas of the HA wells) were used for automated scanning analysis and quantification. The means of total $TRAP^+$ multinucleated cells per unit area and total surface area of $TRAP^+$ multinucleated cells were then calculated after subtracting averaged background signals of the negative control. To quantify the total surface area of resorptive pits in the selected fields, cells were stripped with 1 N NaOH for 16 h, after which the images of eroded bone or HA surfaces were captured as described above.

Oral inoculation of mice with *A. actinomycetemcomitans*. *A. actinomycetemcomitans* strain JP2 (ATCC 29523) was originally purchased from the American Type Culture Collection (Rockville, MD) and grown anaerobically (80% N_2, 10% H_2, 10% CO_2) in tryptic soy broth-yeast extract culture broth (Sigma Chemical, St. Louis, MO) supplemented with 0.75% glucose and 0.4% $NaHCO_3$. Experimental mice, including BALB/c, NOD, NOR, and humanized NOD/SCID, were orally inoculated with fresh *A. actinomycetemcomitans* (10^9 CFU/100 μl of broth mixed with 2% carboxy-methylcellulose in PBS) twice per week for three consecutive weeks as described previously (27). Mice were then sacrificed at week 7 or 8. Age-matched NOD mice without bacterial inoculation served as controls and were kept under the same specific-pathogen-free environmental conditions. The protocol of IFN-γ administration into HuPBL-NOD/SCID mice was used in some experiments, resulting in significantly increased alveolar bone loss in vivo, and has been described previously (49, 54).

qRT-PCR and immunoblot assays for mRNA and protein expression of SOCS and MAPK family molecules. Quantitative reverse transcription-PCR (qRT-PCR) and immunoblot analyses were employed using cells prepared from local cervical lymph nodes and/or the periodontal tissues of *A. actinomyctemcomitans*-inoculated prediabetic, nondiabetic, diabetic NOD mice, and HuPBL-NOD/SCID mice (10 to 16 mice per donor group) whose autologous HuPBL were obtained from individual AgP patients. Total RNA was isolated from cells by using the RNeasy kit (Qiagen) according to the manufacturer's instructions. All RNA samples were DNase treated with DNA-free prior to cDNA synthesis. Digested RNA was reverse transcribed by oligo(dT) priming with reverse transcriptase (SuperScript; Invitrogen). qRT-PCR was performed in duplicates using iCycler and RT^2 real-time SYBR green PCR master mix (SuperArray; Bio-Rad Laboratories) according to the manufacturer's instructions, with optimization of primer and probe concentrations. Primers were designed using the published gene sequences from the GenBank database (National Center for Biotechnology Information) and published literature, including mouse and human SOCS1, SOCS3, SOCS5, TRAF6, mitogen-activated protein kinase (MAPK) family molecules and specific primers for dominant negative SOCS3 (7, 13, 21, 30, 33, 34, 57, 63). The expression of individual genes was calculated by a standard curve method and normalized to the expression of β-actin as a reference gene. Data are presented on a log scale of the change in relative expression. To this end, several master mixes were prepared with different amounts of primers (i.e., 0.05 to 0.9 μM) and probes (0.05 to 0.25 μM) in the presence of AmpliTaq Gold DNA polymerase, AmpErase UNG, deoxynucleoside triphosphates and dUTP, passive reference 1, and optimized buffer. The final mix included a total of 25 μl of 2× master mix, 3 μl DNA template, primers, probe solutions, and sterile water to adjust the volume. RT-PCRs were typically executed for 30 cycles as follows: 2 min at 50°C, 10 min at 95°C, and 35 cycles of 15 s at 95°C and 1 min at 60°C. The cycle threshold (C_T) determinations were repeated for reproducibility. Means and standard deviations were calculated for coefficients of variance for each DNA concentration for which reliability analyses were carried out. Quantification of the samples was accomplished by using a reference standard curve generated from known concentrations of β-actin DNA using the C_T at which fluorescent intensity of each reaction mixture was 3 standard deviations above the background fluorescence.

To quantify protein expression, immunoblot assays were employed as described previously (50, 51). Briefly, the cells/tissues were homogenized in lysis buffer (20 mM Tris HCl, pH 7.4, 150 mM NaCl, 0.5% Triton X-100, 100 μM sodium vanadate, 1 mM dithiothreitol, 5 mg/ml leupeptin, 1 mM phenylmethylsulfonyl fluoride, and protease inhibitor cocktail; Roche Applied Science) and cleared by centrifugation at $15,000 \times g$ at 4°C for 15 min. The extracts were diluted to a 2-mg/ml protein concentration. Equal amounts of cell lysates were separated by 12% sodium dodecyl sulfate-polyacrylamide gel electrophoresis gels via electrophoresis and transferred to polyvinylidene difluoride membranes. Membranes were then blocked with Tris-buffered saline–Tween (TBST; 20 mM Tris-HCl, pH 7.5, 150 mM NaCl, 0.1% Tween 20) containing 5% skim milk and 0.1% Tween 20 in PBS, followed by 2-h incubation with primary MAb, diluted 1/1,000 in buffer. Total protein levels were assessed by using antibodies against the mouse and human SOCS1, SOCS3, SOCS5, TRAF6, Erk, JNK1, p38, Akt, and Myc purchased commercially (R&D Systems, Cell Signaling Technology, and Santa Cruz Biotechnology). Replicate membranes were blotted for the phosphorylated protein species with antibodies against phospho-Erk (Thr202/Tyr204), phospho-Jnk1/2 (Tyr183/185), phospho-p38 (Thr180/Tyr182), and phospho-Akt (Ser473) (Cell Signaling Technology and Santa Cruz Biotechnology). Later, horseradish peroxidase- or allophycocyanin-conjugated anti-mouse or rabbit/rat IgG was used as secondary Ab at a 1/2,000 dilution (47, 48). Bound protein complexes were detected with the enhanced chemiluminescence kit (Amersham) and then visualized with the Kodak-2000 mm Image Station for quantification and comparisons (50, 51). The results of our pilot immunoblot assays suggested that the antibodies used here were specific and did not cross-react or bind nonspecifically to the target molecules (data not shown).

Ad and transfection of $CD11c^+$ DCs in vitro. A recombinant replication-deficient adenoviral (Ad) vector (E1 and E3 deleted) containing myc-tagged wild-type (WT) SOCS3 or a dominant negative (DN) form of SOCS3 cDNA with bacterial β-galactosidase cDNA driven by the CAG promoter (chicken β-actin promoter and cytomegalovirus enhancer) described previously was used in this study (kindly provided by A. Yoshimura, Kyushu University, Japan) (30, 35, 42, 43). The individual Ad-WT-SOC3 or Ad-DN-SOCS3 construct was prepared from homologous recombination in HEK 293 cells (30, 35, 42, 43) containing Ad-E1 gene sequences required for high titers of recombinant virus for production (via the CsCl gradient method) and titer determinations by plaque-forming assay (in PFU) as described previously. The number of viral particles per cell was expressed as the multiplicity of infection (>50 to 100). The virus was stored at −80°C until use. Transfection efficiency was measured via the LacZ/5-bromo-4-chloro-3-indolyl-β-D-galactopyranoside reporter system (data not shown), and SOCS expression was separately confirmed by qRT-PCR and immunoblotting. Ad-DN-SOCS3 (F25A) carries a point mutation in the KIR of SOCS3 was previously reported to enable inhibition of the signaling of WT-SOCS3 via a DN effect (30, 42). This vector system allows reliable gene delivery with high expression in nondividing cells, like DCs, where the Ad carrying DN-SOCS3 sequences yielded almost null protein expression (see Fig. 3A, below).

For DC transfection, Ad alone or Ad-WT-SOCS3 or Ad-DN-SOCS3 cNDA was individually applied to infect $CD11c^+$ DCs generated from total BM cultures of the diabetic NOD mice (or the control species) on day 5 to 6 (in 4 μg/ml polybrene) and repeated once the next day. Transduced $CD11c^+$ DCs (efficiency of ≥50% from LacZ expression) were then enriched and purified via MACS on day 7 (purity and viability, >96%) (1). Other study groups have included the diabetic $CD11c^+$ DCs transduced by Ad alone as a background control for transfection, $CD11c^+$ DCs of BALB/c mice as a positive control, $CD11c^+$ DCs of nondiabetic NOD versus NOR mice as the background control, and DCs only and DCs plus T cells as the negative controls. All DC transduction assays were repeated at least two to three times to ensure reproducibility. However, sufficient quantities of leukocytes were not available from HuPBL-NOD/SCID mice to allow purification of human $CD11c^+$ DCs for parallel study with statistical significance, and thus this was not pursued in the present study. Later, SOCS3 expression was confirmed by qRT-PCR and immunoblotting.

Measurement of alveolar bone loss via digital histomorphometry. Mouse jaw samples were defleshed and stained with methylene blue to define the area between the cementum-enamel junction and the alveolar bone crest. The surface areas represent measurements of the total amount of alveolar bone loss on the

jaws, in square micrometers, which was carried out with a calibrated Leica MZ_{95} stereomicroscope and a Hamamatsu Orca digital camera. The jaw images were captured under 16× magnification; the right and left maxillary first two molars (i.e., M1 and M2) perpendicular to the optical light source were scanned and automatically enumerated by using the density slice features of OpenLab for full quantitation as described previously (14, 27, 49, 54). The results of alveolar bone loss detected in the present study were consistent with our previous findings using the immunocompetent BALB/c, diabetic NOD, and humanized NOD/SCID mice, where active alveolar bone loss and/or significantly inflamed periodontal lesions did not occur until 7 to 8 weeks post-*A. actinomycetemcomitans* inoculation (27, 49, 54); therefore + signs were used to depict the magnitudes of alveolar bone loss from low (+) to high (+++).

Statistical analysis. Statistical analysis was performed using a two-sided Student *t* test, and the difference between various groups was considered statistically significant when the *P* value was <0.05.

RESULTS

Increased SOCS1, SOCS3, and SOCS5 expression is associated with higher alveolar bone loss in diabetic NOD and IFN-γ-treated humanized NOD/SCID mice in vivo. First, to assess the expression profiles of critical SOCS molecules (namely, 1, 3, and 5) in active periodontal lesions with alveolar bone loss, diabetic versus control NOD, and IFN-γ-treated versus sham-treated HuPBL-NOD/SCID mice described previously (14, 27, 49, 54) were employed for our study here. Through previously established protocols (14, 27, 49, 54), *A. actinomycetemcomitans*-reactive $CD4^+$ T cells were purified from cervical lymph nodes of prediabetic, nondiabetic, diabetic NOD, and diabetic NOD mice treated with or without OPG ($n = 5$ to 6 mice/group) versus sham-treated (N1 to N3) or IFN-γ-treated (T1 to T4) HuPBL-NOD/SCID mice ($n = 10$ to 16 mice/group), respectively. The results of qRT-PCR and immunoblot analyses showed significantly increased SOCS1, SOCS3, and SOCS5 mRNA and protein expression levels in *A. actinomycetemcomitans*-reactive RANKL-expressing $CD4^+$ T cells from diabetic NOD and IFN-γ-treated HuPBL-NOD/SCID mice (Fig. 1A and B), which closely correlates with the enhanced alveolar bone loss post-microbial challenge in vivo (Fig. 1A and B), based on previously reported results (27, 49, 54). These findings are consistent with those of Taubman's and Garlet's, in which rat SOCS1 and SOCS5 mRNA and protein levels versus human SOCS1, -2, and -3 mRNA levels were increased in vivo postchallenge by DNA of *Porphyromonas gingivalis* in diseased periodontal tissues compared to healthy controls (12, 47). Given the suppressive nature of SOCS family molecules and their roles in controlling cytokine receptor signaling, it is conceivable that SOCS1, -3, and -5 are likely engaged in modulating the inflammatory responses during periodontal infections. In particular, we were interested in studying the SOCS3 molecule, which has been previously shown to modulate inflammation-induced osteoclastogenesis and bone loss in vitro and in experimental rheumatoid arthritis models in vivo (11, 35, 43, 60–62).

Higher SOCS3 expression in $CD11c^+$ DC–T-cell–*A. actinomycetemcomitans* cocultures is strongly associated with enhanced osteoclastogenesis for bone resorption in vitro. DCs and T cells are known to infiltrate the periodontal lesions and form aggregates at disease sites, thereby affecting disease pathogenesis and alveolar bone loss. To investigate the link between SOCS3 expression and inflammation-induced osteoclastogenesis, we utilized our recently described RANKL-dependent DDOC coculture system, where immature $CD11c^+$ DCs can develop into TRAP-expressing functional OCs capable of resorbing bone substrates after incubation with $CD4^+$ T cells and activating signals such as the microbial or protein Ags (i.e., *A. actinomycetemcomitans*) (1–3). BM-derived $CD11c^+$ DCs were prepared from NOD mice and were cocultured with 0.5×10^6 syngeneic $CD4^+$ T cells and sonicate of *A. actinomyctemcomitans* for 4 to 5 days before qRT-PCR, Western blotting, and TRAP staining for quantification as previously described (1, 2). Upon comparing all the different groups, we found that diabetic NOD mice cocultures had noticeably higher levels of SOCS3 mRNA and protein expression by qRT-PCR and immunoblotting, compared to prediabetic and nondiabetic mice (Fig. 2A). In parallel, diabetic NOD mice $CD11c^+$ DC cocultures exhibited significantly higher TRAP activity (Fig. 2B) and bone resorption (which mirrored TRAP results [thus, data are not shown]), compared to prediabetic and nondiabetic cocultures. These findings correlate SOCS3 expression to RANKL-mediated osteoclastogenesis and bone loss, in diabetic NOD mouse cells in vitro, thereby establishing a potential role for SOCS3 in the regulation of inflammation-induced osteoclastogenesis and bone loss in response to the challenge by a periodontal pathogen.

Expression of a dominant-negative form of the SOCS3 gene in $CD11c^+$ DCs significantly reduces RANKL-mediated osteoclastogenesis and bone resorption during immune interactions with $CD4^+$ T cells and *A. actinomycetemcomitans* in vitro. To further test the role of SOCS3 during DDOC-associated osteoclastogenesis and inflammation-induced bone loss, we employed a reductionist approach by using a well-established Ad construct to knock down its function in $CD11c^+$ DCs by transfecting them with a DN SOCS3 prior to their coculture with syngeneic $CD4^+$ T cells, thereby allowing reliable gene delivery with high expression in DC. To this end, total BM cells from various groups of mice were cultured with IL-4 plus GM-CSF for 5 to 6 days and were then subjected to a transfection protocol with Ad (+LacZ) alone or Ad-WT-SOCS3 (or DN-SOCS3) cDNA, which was repeated once again the next day. On day 7, transfected $CD11c^+$ DCs were separated by MACS as described previously (1) followed by coculturing with 0.5×10^6 syngeneic $CD4^+$ T cells (1:1 ratio) and *A. actinomycetemcomitans* for 4 to 5 days before TRAP staining and quantification. This DN-SOCS3 Ad construct, F25A, carrying a point mutation in the KIR of WT SOCS3, has been shown to enable inhibition of the signaling of functional SOCS3 via a DN effect (30, 42). In our study, DN-SOCS3 in vitro knockdown was effective since (i) both WT and DN Ad constructs had similar levels of resulting SOCS3 mRNA expression and overall Ad-specific myc expression levels via qRT-PCR and immunoblot analyses, respectively, and (ii) transfection with Ad-DN-SOCS3 resulted in a significant reduction of WT-SOCS3 protein expression (Fig. 3A and B). We noted that the anti-SOCS3 Ab employed only detected WT protein and not the mutant DN-SOCS3 form (Fig. 3B and data not shown). Subsequently, when we assessed the effects of DN-SOCS3 expression in $CD11c^+$ DCs of diabetic NOD mice for inflammation-induced osteoclastogenesis, the results of such a loss-of-function analysis showed that there was a significant reduction in TRAP activity (Fig. 3C) and bone resorption (with mirrored TRAP results [thus, data are not shown]). Interestingly, we also found that the reduced DDOC-associated osteoclastogenesis and bone loss in DN-SOCS3-transfected DC cocultures were compa-

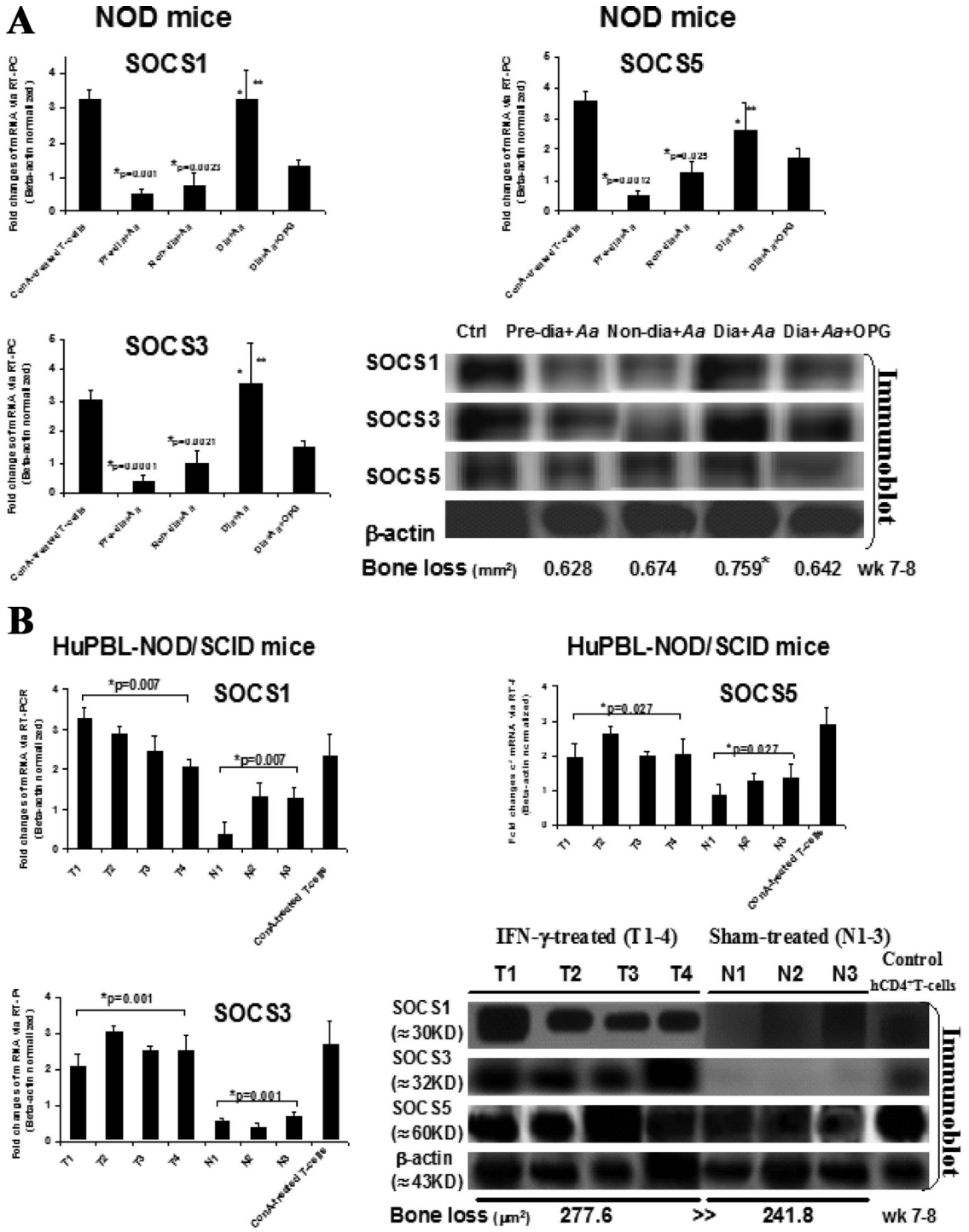

FIG. 1. Increased expression of SOCS1, SOCS3, and SOCS5 mRNA and proteins is associated with higher alveolar bone loss in vivo. $CD4^+$ T cells were purified from cervical lymph nodes of prediabetic, nondiabetic, and diabetic NOD mice with or without OPG treatment (n = 5 to 6 mice/group) versus sham-treated (N1 to N3) or IFN-γ-treated (T1 to T4) HuPBL-NOD/SCID mice (n = 10 to 16 mice/group) post-oral infection with *A. actinocytmecomitans*. qRT-PCR and immunoblot analyses were employed to detect SOCS1, -3, and -5 mRNA and protein versus phosphor-protein expression levels, using ConA-treated $CD4^+$ T cells as a positive control. SOCS1, SOCS3, and SOCS5 mRNA and protein expression levels in diabetic, prediabetic, and nondiabetic NOD mice (A) and in IFN-γ-treated HuPBL-NOD/SCID (T1 to T4) versus sham-treated mice (N1 to N3) (B). The results of qRT-PCR are presented after normalization to β-actin expression levels and are representative of ≥2 to 3 independent studies with similar results. Mean alveolar bone loss in both mouse models was reported previously (27, 54) and is summarized at the bottom of panels A and B.

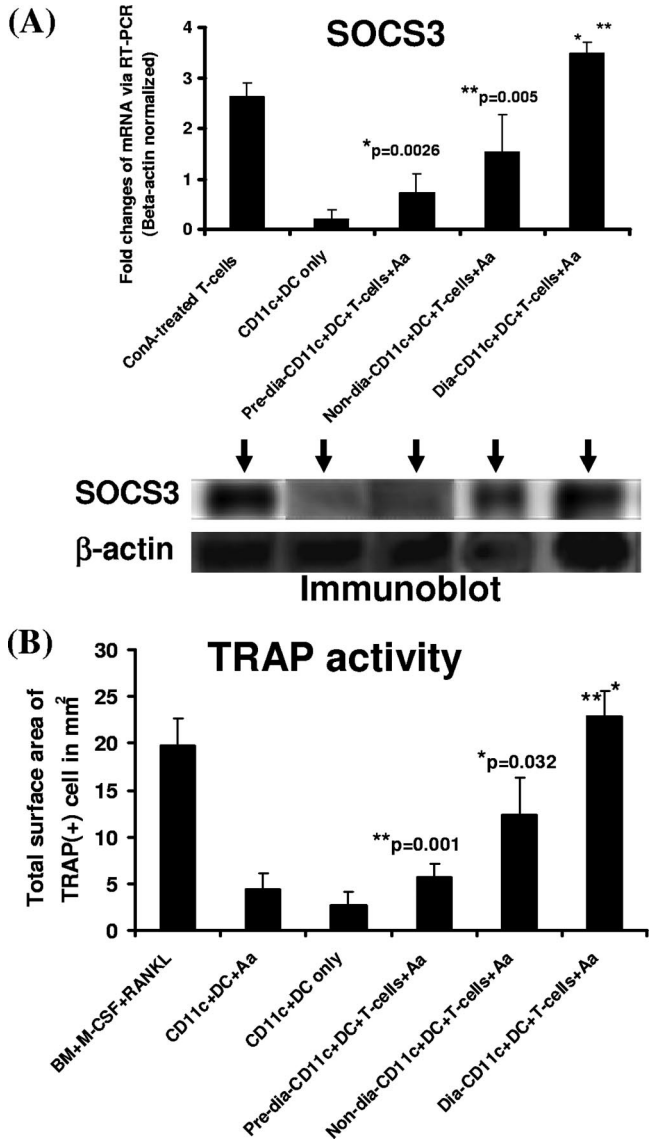

FIG. 2. Increased SOCS3 expression in diabetic $CD11c^+$ DCs is strongly associated with higher osteoclastogenesis and bone resorption in vitro. A total of 0.5×10^6 BM-derived immature $CD11c^+$ DCs prepared from the femurs of diabetic, prediabetic, and nondiabetic NOD mice were cocultured for 4 to 5 days with syngeneic naïve (0.5×10^6) $CD4^+$ T cells, and the sonicated Ag of *A. actinomyctemcomitans* (Aa). BALB/c total BM cells cultured with M-CSF and RANKL and BM-derived $CD11c^+$ DCs cultured with *A. actinomyctemcomitans* were used as positive controls. The cells were then collected on day 4 or 5 and used for the preparation of RNA and cell lysates for subsequent qRT-PCR and Western blot analyses. Representative data from ≥2 to 3 independent experiments are presented here, with SOCS3 mRNA and protein expression levels (A) and TRAP activity (B) shown from the diabetic, nondiabetic, and prediabetic NOD mice. The results of bone resorption mirrored those of TRAP activity and thus are not shown here.

rable to those of nondiabetic NOD versus NOR mice (Fig. 3D and data not shown). The same diabetic $CD11c^+$ DCs transduced by Ad vector or Ad-WT-SOCS3 maintained comparable levels of TRAP and bone resorption activities as WT $CD11c^+$ DCs (Fig. 3D). Collectively, these data suggest that SOCS3 can modulate RANKL-mediated osteoclastogenesis and bone loss via DC–T-cell immune interactions at least in vitro.

Elevated SOCS1, SOCS3, and SOCS5 expression levels in vivo are not associated with changes in TRAF6 and MAPK adaptor protein expression. We previously showed that the inflammatory cytokine IFN-γ is coexpressed with RANKL in *A. actinomycetemcomitans*-reactive $CD4^+$ T cells, where it positively modulates osteoclastogenesis and enhances active alveolar bone loss in vivo (54). This phenomenon was also evident in *A. actinomycetemcomitans*-associated alveolar bone loss mediated by a potent proapoptotic antigen (i.e., CagE homologue) (50, 51), which induces robust IFN-γ expression in microbe-specific $RANKL^+$ Th1 cells (27, 54). In contrast, IL-10 in our model exerts an antiinflammatory effect by downregulating RANKL-mediated osteoclastogenesis both in vivo and in vitro, suggesting that there is a network of regulatory interactions between RANKL and immune cytokines in the periodontium (53, 63). To investigate the early effector molecules downstream of inflammatory cytokine signaling associated with osteoclastogenesis, we examined the mRNA and protein (and phosphor-protein) expression profiles of key adaptors, including TRAF6 and the well-known MAPK signaling molecules (i.e., Erk, Junk1, p38, and Akt) (21, 31, 55, 58). For this, *A. actinomycetemcomitans*-reactive $CD4^+$ T cells were purified from cervical lymph nodes of prediabetic, nondiabetic, diabetic NOD, and diabetic NOD mice treated with OPG compared to sham-treated (N1 to N3) or IFN-γ-treated (T1 to T4) HuPBL-NOD/SCID mice, respectively. The results of qRT-PCR and immunoblot analyses of the purified cells and cell lysates revealed no significant differences in TRAF6 mRNA or protein expression levels in *A. actinomycetemcomitans*-reactive RANKL-expressing $CD4^+$ T cells prepared from diabetic, prediabetic, or nondiabetic NOD mice versus IFN-γ- or sham-treated HuPBL-NOD/SCID mice (Fig. 4A), despite the significant difference in alveolar bone loss detected in vivo. Moreover, when comparing immunoblots of IFN-γ versus sham-treated *A. actinomycetemcomitans*-infected HuPBL-NOD/SCID T cells, we found no detectable significant difference in the expression of MAPK signaling molecules (i.e., Erk, Junk1, p38, and Akt) (Fig. 4B). Such measurement of TRAF6 and MAPK protein versus phosphorylated protein expression levels were very similar and the results did not change even when using samples from periodontal lesions at different time points (i.e., weeks 6 to 8) (14, 27, 28, 54). Considering the importance and complexity of DC and T-cell interactions during disease pathogenesis and our observations shown in Fig. 4, it is speculated that (i) ubiquitin-mediated degradation of TRAF6 protein may not be the only target/event associated with SOCS3-induced distal signaling (or other SOCS family members), and (ii) there is likely another adaptor complex(es) involved in the SOCS3-induced downstream effect on osteoclastogenesis in $RANKL^+$ T cells and/or DDOC.

DISCUSSION

SOCS family molecules are involved in the regulation of the functions and activities of both T cells and APCs (i.e., DCs) (9, 11, 35, 42, 43, 60–62). Recent studies provide ample evidence that SOCS3, in particular, may determine the nature and functions of cytokines signaling by tuning up or down the inhibitory effect of proinflammatory cytokines during RANKL-mediated

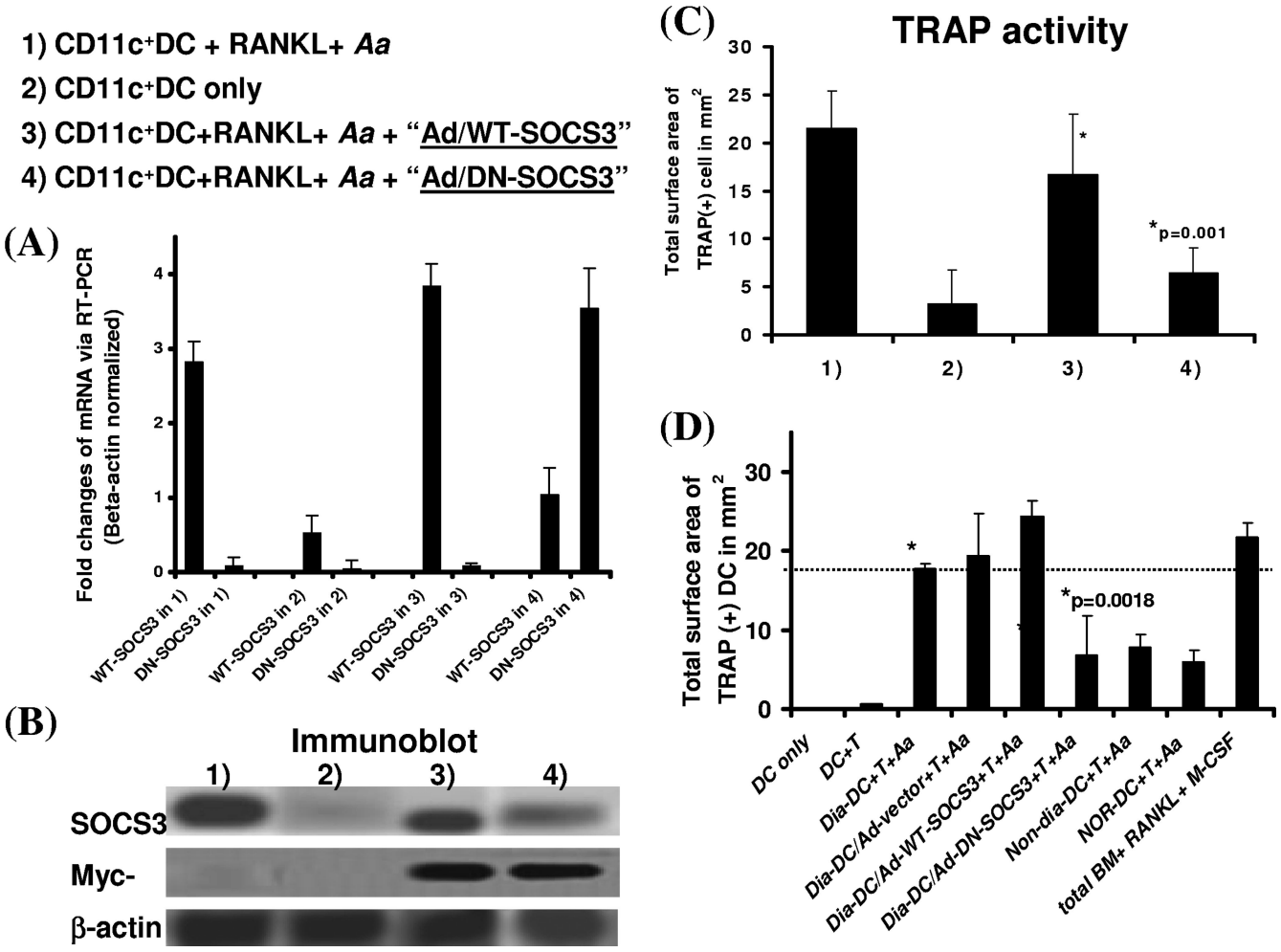

FIG. 3. Knocking down functional SOCS3 in CD11c$^+$ DCs abrogates RANKL-mediated osteoclastogenesis and bone resorption during immune interactions with CD4$^+$ T cells in response to *A. actinomycetemcomitans* sonicated Ags in vitro. Total BM cells of BALB/c, NOD (e.g., diabetic, prediabetic, or nondiabetic) or NOR mice were cultured with IL-4 plus GM-CSF. On day 5, BM cultures were subjected to a transfection protocol with Ad (+LacZ) alone or Ad-WT-SOCS3 (or DN-SOCS3) cDNA (DN with F25A mutation with a loss of function) and repeated once again on day 6. On day 7, CD11c$^+$ DCs were separated by MACS and then cocultured with syngeneic CD4$^+$ T cells (1:1 ratio) and *A. actinomyctemcomitans* for 4 to 5 days before TRAP staining and quantification. Later, cocultured cells were collected and split for the preparation of RNA and cell lysates for subsequent qRT-PCR and immunoblot analyses. Splenocytes plus ConA and total BM plus RANKL plus M-CSF were used as positive controls, while DC-only and DCs plus T cells served as the negative controls. (A) Results after transfection with Ad-DN-SOCS3 or Ad-WT-SOCS3, the results of qRT-PCR for SOCS3 expression levels; (B) immunoblots for SOCS3 protein expression levels. (C and D) The results of TRAP activity analysis. The data for bone resorption mirrored those of TRAP activity and thus are not shown here. The data shown are representative of ≥2 to 3 independent studies.

osteoclastogenesis (45, 63). Although reports have suggested the contribution of SOCS during inflammation to cytokine signaling networks associated with innate and adaptive immunity (62), the roles of individual SOCS family molecules (e.g., SOCS1, -3, and -5) (12, 47) during periodontal pathogenesis remain unclear. In the present study, we employed the established mouse models to investigate the osteo-immune interactions during periodontal pathogenesis and bone loss, comparing the nondiabetic versus diabetic and the humanized NOD/SCID systems. The models used in this report provide robust systems to study disease pathogenesis during host-microbe interactions and alveolar bone loss. However, due to the complex nature of type 1 diabetes and the osteo-immune interactions involved (27), it is cautioned that some limitations may apply for interpreting the role of SOCS3 in regulating alveolar bone loss in people with diabetic conditions. With that in mind, we demonstrated that higher SOCS1, SOCS3, and SOCS5 expression levels are associated with RANKL-mediated alveolar bone loss and enhanced CD11c$^+$ DC-derived osteoclastogenesis in vivo and in vitro, respectively. More interestingly, we were able to show that reduced expression of functional SOCS3 in CD11c$^+$ DCs results in significantly lower osteoclastogenesis and DDOC development during immune interactions with T cells, based on TRAP expression and bone resorptive activity. Similar observations were described by Ohishi et al. using BM-derived Mo as the classical (TRAP$^+$) OC precursors (35). In that study, SOCS3 expression was upregulated upon RANKL treatment, whereas TRAP$^+$ OC precursor frequency is significantly reduced in SOCS3-deficient mice.

Herein, we detected increased SOCS3 expression in both

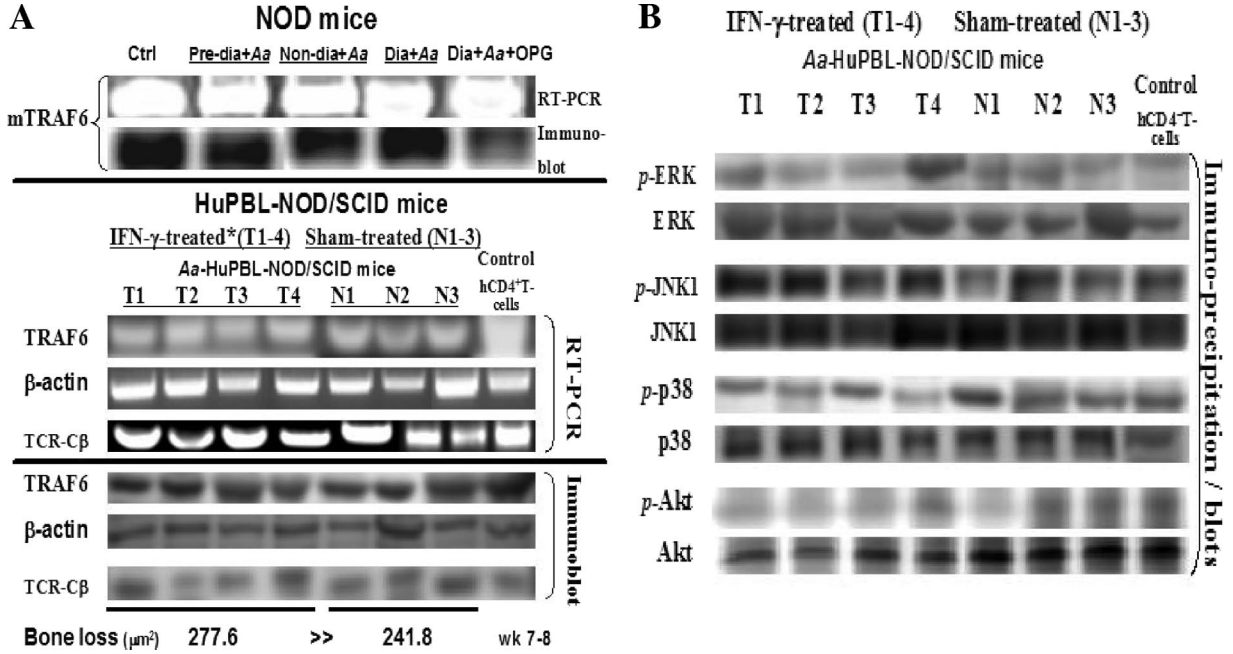

FIG. 4. Elevated SOCS1, SOCS3, and SOCS5 expression levels are not associated with changes in TRAF6 and MAPK adaptor expression. $CD4^+$ T cells were purified from cervical lymph nodes of prediabetic, nondiabetic, and diabetic NOD mice with or without OPG and compared to sham-treated (N1 to N3) or IFN-γ-treated (T1 to T4) HuPBL-NOD/SCID mice with *A. actinomycetemcomitans*-induced periodontitis. qRT-PCR and immunoblot analyses were employed for detection and quantification of TRAF-6, ERK, JNK1, p38, and Akt mRNA and protein/phosphor-protein expression levels, respectively (A and B). The resulting data from the qRT-PCR were normalized to those of β-actin and/or TCR-Cβ mRNA expression levels. Magnitudes of alveolar bone loss in NOD versus HuPBL-NOD/SCID mouse models in vivo are depicted and shown as the averaged means. The results showed that there were no significant statistical differences in TRAF6 mRNA and proteins and phosphorylated proteins ($P > 0.05$ for all cases) (TRAF6 and MAPK signaling adaptors included Erk, Jnk1, p38, and Akt) being expressed by *A. actinomycetemcomitans*-reactive RANKL-expressing $CD4^+$ T cells during alveolar bone loss in NOD versus HuPBL-NOD/SCID mouse models in vivo (as reflected by the number of + symbols for bone loss depicted in panel A) (27). Mean alveolar bone loss in vivo had been reported previously (54) and is summarized at the bottom of panel A. Statistical significance was assessed by the paired Student's *t* test and the differences were considered not significant at a *P* level of >0.05. The data shown here are representative of >2 to 3 independent studies.

microbe-reactive $CD4^+$ T cells of diabetic mice (Fig. 1) and DC–T-cells–*A. actinomycetemcomitans* cocultures (Fig. 2), which clearly correlated with the increased alveolar bone loss detected in the animals. We focused our study on the "direct" impact of SOCS3 expression in $CD11c^+$ DCs, as the OC precursors, on inflammation-induced osteoclastogenesis by monitoring the development of $TRAP^+$ multinucleated DDOC in response to RANKL produced by T cells upon their activation in cocultures. It remains unclear, but is of high interest, whether SOCS3 expression in DCs plays a more important role than in T cells regarding its regulation of inflammation-induced osteoclastogenesis. While this issue is under investigation, we anticipate that the influence of SOCS3 expression in $CD4^+$ T cells and its effects on the resulting cytokine profiles and subsequent osteoclastogenesis during DC–T-cell interactions will likely be much more complicated (52, 53). Meanwhile, it is noteworthy that OPG treatment in *A. actinomycetemcomitans*-infected diabetic NOD mice was employed here as an additional control (Fig. 1A), because it yielded a robust reduction of alveolar bone loss in our previous study (27). Whether or not OPG can regulate any SOCS activity associated with bone loss is beyond the scope of the present study, and it will be addressed in future studies.

It is suggested that there are (i) differential thresholds for the sensitivities of different cell types (i.e., Mo/MQ, lymphocytes, mesenchymal cells, etc.) via SOCS3 regulation (or other SOCS), (ii) different adaptor complexes involved in the regulation of SOCS downstream effects, and (iii) RANKL and cytokine interaction networks signal to fine-tune the outcomes of SOCS regulation (8, 10, 11, 35, 43, 53, 60–62). SOCS molecules were previously thought to regulate cytokine signaling (particularly in T cells) and, consequently, to influence the inflammation-induced bone loss. In particular, SOCS can act downstream of both Th1 (e.g., TNF-α, IL-1, and IFN-γ) and Th2 (e.g., IL-4) cytokines that promote and inhibit inflammation-induced bone loss, respectively (35, 42, 60–62). In addition, several reports have indicated a negative role for SOCS1 and SOCS3 in the regulation of human versus experimental periodontitis- and arthritis-associated inflammation (12, 43, 60); however, the direct contribution of specific SOCS to regulating the inflammation-induced osteoclastogenesis and bone loss has not been shown. Therefore, any conclusions drawn require careful interpretations, as the interactions among various cell types (i.e., Mo, MQ, T cells, granulocytes, etc.) of the inflammatory infiltrates during disease pathogenesis are complex. Nevertheless, our present findings support a positive contribution of SOCS3 to DC-derived osteoclastogenesis. This highlights an interesting and previously unknown role of SOCS3 during the osteo-immune interactions under inflammation, therefore providing important insights into the regulatory mechanisms of immune

mediators in bone homeostasis under normal versus pathological conditions, such as periodontal infection associated with type 1 diabetes (27). Our data are also in accordance with the recent study by Wormald et al., in which higher levels of SOCS expression (i.e., 1, 3, or 5) were strongly associated with the diseased periodontal tissues in the presence of (pro)inflammatory cytokines (e.g., RANKL, IL-1, and IL-6) (12, 35, 47). Further, particular SOCS molecules can be "hard-wired" to specific cytokine signaling pathways, thereby allowing them to modulate the kinetics of downstream effects (61). In light of the above findings, it is conceivable that SOCS3 may affect Toll-like receptor signaling, thereby affecting the expression of pro- and/or antiinflammatory cytokines (i.e., IFN-γ, IL-10, etc.) via specific JAK/STAT pathways.

The molecular mechanisms underlying the differential qualitative and/or quantitative regulation of STAT activation distal to SOCS signaling remain unclear to date, because how individual SOCS molecules execute such regulation during DC–T-cell interactions will require further study. Based on our findings shown in Fig. 4, we speculate that the ubiquitin-mediated degradation of TRAF6 protein may not be the only target and/or event associated with SOCS3-associated regulation. Moreover, we anticipate that the possible candidates include the adaptors associated with a signaling complex of IL-1R/TAK1, ITAM, TNF receptor, and type I IFN- receptor, while other immune receptors, (e.g., CD40, IL-6, IL-12, etc.) may also be involved (19, 22, 35, 42, 43, 45, 58, 60–62). Interestingly enough, SOCS3 has been recently suggested to promote RANKL-dependent Mo/MQ-mediated osteoclastogenesis via signaling the transforming growth factor β downstream pathway in vitro (10).

In summary, our study provides clear evidence that SOCS3 is a critical player in RANKL-mediated osteoclastogenesis during DC–T-cell interactions associated with periodontal inflammation leading to severe alveolar bone loss as seen in diabetes. We also reveal that in response to inflammatory cytokines such as IFN-γ, an early effector(s) downstream of RANKL-RANK signaling may be modulated by SOCS3, thereby influencing bone homeostasis under pathological conditions via pathways independent of those previously described (8, 19, 22, 35, 41–43, 45, 60, 62). For instance, the existence of a TRAF6-independent pathway and non-STAT1 family molecules involved in NF-κB and/or Jun N-terminal protein kinase pathways for osteoclastogenesis have been described (20, 24, 39). Our latest experiments using microarrays and qRT-PCR analyses of $CD11c^+$ DC-derived OCs further suggest that a non-TRAF6 signaling complex is likely associated with the enhanced osteoclastogenesis studied here (Fig. 1 and unpublished data) (40). These findings point to the possible involvement of an additional signaling adaptor(s) closely linked to SOCS3-mediated regulation of osteoclastogenesis during DC–T-cell immune interactions that is not associated with RANK-TRAF6 and the MAPK axis (i.e., Erk, Jun, p38, etc.). However, whether this is indeed the case remains to be further studied. The cytokine signaling networks at the osteo-immune interface are intricate; thus, further understanding of the in vivo effects of SOCS3 signaling is essential to gain important insights into the regulatory mechanisms of immune mediators during bone homeostasis in health and disease.

ACKNOWLEDGMENTS

This work was supported in part by research grants from the Eastman Dental Center, University of Rochester, Rochester, NY, and the National Institutes of Health (DE15786 and DE018356 to Y.-T.A.T.).

REFERENCES

1. **Alnaeeli, M., J. M. Penninger, and Y.-T. A. Teng.** 2006. Immune interactions with $CD4^+$ T cells promote the development of functional osteoclasts from murine $CD11c^+$ dendritic cells. J. Immunol. **177:**3314–3326.
2. **Alnaeeli, M., J. Park, D. Mahamed, J. M. Penninger, and Y.-T. A. Teng.** 2007. Dendritic cells at the osteo-immune interface: implications for inflammation-induced bone loss. J. Bone Miner. Res. **22:**775–780.
3. **Alnaeeli, M., and Y.-T. A. Teng.** 2009. Dendritic cells differentiate into osteoclasts in bone marrow microenvironment *in vivo*. Blood **113:**264–265.
4. **Alnaeeli, M., and Y.-T. A. Teng.** Dendritic cells: a new player in osteoimmunology. Curr. Mol. Med., in press.
5. **Arron, J. R., and Y. Choi.** 2000. Osteoimmunology: bone versus immune system. Nature **408:**535–536.
6. **Bostanci, N., T. Ilgenli, G. Emingil, B. Afacan, B. Han, H. Toz, G. Atilla, F. J. Hughes, and G. N. Belibasakis.** 2007. Gingival crevicular fluid levels of RANKL and OPG in periodontal diseases: implications of their relative ratio. J. Clin. Periodontol. **34:**370–376.
7. **Brender, C., R. Columbus, D. Metcalf, E. Handman, R. Starr, N. Huntington, D. Tarlinton, N. Ødum, S. E. Nicholson, N. A. Nicola, D. J. Hilton, and W. S. Alexander.** 2004. SOCS5 is expressed in primary B and T lymphoid cells but is dispensable for lymphocyte production and function. Mol. Cell. Biol. **24:**6094–6103.
8. **Chen, Z., A. Leurence, Y. Kanno, M. Pacher-Zavisin, B-M. Zhu, C. Tato, A. Yoshimura, L. Hennighausen, and J. O'Shea.** 2006. Selective regulatory function of Socs3 in the formation of IL-17-secreting T cells. Proc. Natl. Acad. Sci. USA **103:**8137–8142.
9. **Cutler, C. W., and Y.-T. A. Teng.** 2007. Oral mucosal dendritic cells and periodontitis: many sides of the same coin with new twists. Periodontology **45:**35–50.
10. **Fox, S. W., S. Jaharul, H. Alison, C. Lovibond, and T. J. Chambers.** 2003. The possible role of TGF-β-induced suppressors of cytokine signalling expression in osteoclast/macrophage lineage commitment *in vitro*. J. Immunol. **170:**3679–3687.
11. **Frobose, H., S. G. Ronn, P. E. Heding, H. Mendoza, P. Cohen, T. Mandrup-Poulsen, and N. Billestrup.** 2006. Suppressor of cytokine signalling-3 inhibits interleukin-1 signaling by targeting the TRAF-6/TAK-1 complex. Mol. Endocrinol. **20:**1587–1596.
12. **Garlet, G. P., C. R. Cardoso, A. P. Campanelli, W. Martins Jr., and J. S. Silva.** 2006. Expression of suppressors of cytokine signalling in disease periodontal tissues: a stop signal for disease progression? J. Clin. Periodontol. **41:**580–584.
13. **Gomez-Escobar, N., C. Bennett, L. Prieto-Lafuente, T. Aebischer, C. C. Blackburn, and R. M. Maizels.** 2005. Heterologous expression of the filarial nematode *alt* gene products reveals their potential to inhibit immune function. BMC Biol. **3:**8–14.
14. **Graves, D. T., D. Fine, Y.-T. A. Teng, T. E. Van Dyke, and G. Hajishengallis.** 2008. The use of rodent models to investigate host-bacteria interactions related to periodontal diseases. J. Clin. Periodontol. **35:**89–105.
15. **Henderson, B., and S. P. Nair.** 2003. Hard labour: bacterial infection of the skeleton. Trend Microbiol. **11:**570–577.
16. **Hofbauer, L. C., and A. E. Heufelder.** 2001. The role of osteoprotegerin and receptor activator of nuclear factor κB ligand in the pathogenesis and treatment of rheumatoid arthritis. Arthritis Rheum. **44:**253–259.
17. **Hofbauer, L. C., and M. Schoppet.** 2004. Clinical implication of the osteoprotegerin /RANKL/RANK system for bone and vascular diseases. JAMA **28:**490–495.
18. **Honore, P., N. M. Luger, M. A. Sabino, M. J. Schwei, S. D. Rogers, D. B. Mach, P. F. O'Keefe, M. L. Ramnaraine, D. R. Clohisy, and P. W. Mantyh.** 2000. Osteoprotegerin blocks bone cancer-induced skeletal destruction, skeletal pain and pain-related neurochemical reorganization of the spinal cord. Nat. Med. **6:**521–528.
19. **Kaneda, T., T. Nojima, M. Nakagawa, A. Ogasawara, H. Kaneko, T. Sato, H. Mano, M. Kumegawa, and Y. Hakeda.** 2000. Endogenous production of TGF-beta is essential for osteoclastogenesis induced by a combination of receptor activator of NF-kappa B ligand and macrophage-colony stimulating factor. J. Immunol. **165:**4254–4263.
20. **Kim, N., Y. Kadono, M. Takami, J. Lee, S.-H. Lee, F. Okada, J. H. Kim, T. Kobayashi, P. R. Odgren, H. Nakano, W.-C. Yeh, S.-K. Lee, J. A. Lorenzo, and Y. Choi.** 2005. Osteoclast differentiation independent of the TRANCE-RANK-TRAF6 axis. J. Exp. Med. **202:**589–595.
21. **Kobayashi, T., P. T. Walsh, M. C. Walsh, K. M. Speirs, E. Chiffoleau, C. G. King, W. W. Hancock, J. H. Caamano, C. A. Hunter, P. Scott, L. A. Turka, and Y. Choi.** 2003. TRAF6 is a critical factor for dendritic cell maturation and development. Immunity **19:**353–363.
22. **Koga, T., M. Inui, K. Inoue, S. Kim, A. Suematsu, E. Kobayashi, T. Iwata, H. Ohnishi, T. Matozaki, T. Kodama, T. Taniguchi, H. Takayanagi, and T.**

Takai. 2004. Costimulatory signals mediated by the ITAM motif cooperate with RANKL for bone homeostasis. Nature **428:**758–763.
23. **Kong, Y. Y., H. Yoshida, I. Sarosi, H. L. Tan, E. Timms, C. Capparelli, S. Morony, A. J. Oliveira-dos Santos, G. Van, A. Itie, W. Khoo, A. Wakeham, C. R. Dunstan, D. L. Lacey, T. W. Mak, W. J. Boyle, and J. M. Penninger.** 1999. OPGL is a key regulator of osteoclastogenesis, lymphocyte development and lymph-node organogenesis. Nature **397:**315–323.
24. **Kong, Y. Y., U. Feige, I. Sarosi, B. Bolon, A. Tafuri, S. Morony, C. Capparelli, J. Li, R. Elliott, S. McCabe, T. Wong, G. Campagnuolo, E. Moran, E. R. Bogoch, G. Van, L. T. Nguyen, P. S. Ohashi, D. L. Lacey, E. Fish, W. J. Boyle, and J. M. Penninger.** 1999. Activated T cells regulate bone loss and joint destruction in adjuvant arthritis through osteoprotegerin ligand. Nature **402:** 304–308.
25. **Lacey, D. L., E. Timms, H. L. Tan, M. J. Kelley, C. R. Dunstan, T. Burgess, R. Elliott, A. Colombero, G. Elliott, S. Scully, H. Hsu, J. Sullivan, N. Hawkins, E. Davy, C. Capparrelli, A. Eli, Y. X. Qian, S. Kaufman, I. Sarosi, V. Shalhoub, G. Senaldi, J. Guo, J. Delaney, and W. J. Boyle.** 1998. Osteoprotegerin ligand is a cytokine that regulates osteoclast differentiation and activation. Cell **93:**165–176.
26. **Leon, B., M. del Hoyo, V. Parrillas, H. H. Vargas, P. Sanchez-Mateos, N. Longo, M. Lopez-Bravo, and C. Ardavin.** 2004. Dendritic cell differentiation potential of mouse monocytes: monocytes represent immediate precursors of $CD8^-$ and $CD8^+$ splenic dendritic cells. Blood **103:**2668–2676.
27. **Mahamed, D. A., A. Marleau, M. Alnaeeli, B. Singh, X. Zhang, J. M. Penninger, and Y. T. Teng.** 2005. G(-) anaerobes-reactive $CD4^+$ T-cells trigger RANKL-mediated enhanced alveolar bone loss in diabetic NOD mice. Diabetes **54:**1477–1486.
28. **Marleau, A. M., and B. Singh.** 2002. Myeloid dendritic cells in non-obese diabetic mice have elevated costimulatory and T helper-1-inducing abilities. J. Autoimmun. **19:**23–35.
29. **Marleau, A. M., K. L. Summers, and B. Singh.** 2008. Differential contributions of APC subsets to T cell activation in non-obese diabetic mice. J. Immunol. **180:**5235–5249.
30. **Matsumoto, A., Y. Seki, R. Watanabe, K. Hayashi, J. A. Johnston, Y. Harada, R. Abe, A. Yoshimura, and M. Kubo.** 2003. A role of suppressor of cytokine signaling 3 (SOCS3/CIS3/SSI3) in CD28-mediated interleukin 2 production. J. Exp. Med. **197:**425–436.
31. **Matsumoto, M., T. Sudo, T. Saito, H. Osada, and M. Tsujimoto.** 2000. Involvement of p38 mitogen-activated protein kinase signaling pathway in osteoclastogenesis mediated by receptor activator of NF-kappa B ligand (RANKL). J. Biol. Chem. **275:**31155–31161.
32. **Miyamoto, T., O. Ohneda, F. Arai, K. Iwamoto, S. Okada, K. Takagi, D. M. Anderson, and T. Suda.** 2001. Bifurcation of osteoclasts and dendritic cells from common progenitors. Blood **98:**2544–2554.
33. **Morioka, D. T., E. Asilmaz, J. Hu, J. F. Dishinger, A. J. Kurpad, C. F. Elias, H. Li, J. K. Elmquist, R. T. Kennedy, and R. N. Kulkarni.** 2007. Disruption of leptin receptor expression in the pancreas directly affects β cell growth and function in mice. J. Clin. Investig. **117:**2860–2868.
34. **Nishimura, M., and S. Naito.** 2005. Tissue-specific mRNA expression profiles of human Toll-like receptors and related genes. Biol. Pharm. Bull. **28:**886–892.
35. **Ohishi, M., Y. Matsumura, D. Aki, T. Mashima, K. Taniguchi, T. Kobayashi, T. Kukita, Y. Iwamoto, and A. Yoshimura.** 2005. Suppressors of cytokine signalling-1 and -3 regulate osteoclastogenesis in the presence of inflammatory cytokines. J. Immunol. **174:**3024–3031.
36. **Page, R. C., and H. E. Schroeder.** 1976. Pathogenesis of inflammatory periodontal disease. A summary of current work. Lab. Investig. **34:**235–249.
37. **Pihlstrom, B. L., B. S. Michalowicz, and N. W. Johnson.** 2005. Periodontal diseases. Lancet **266:**1809–1820.
38. **Rivollier, A., M. Mazzorana, J. Tebib, M. Piperno, T. Aitsiselmi, C. Rabourdin-Combe, P. Jurdic, and C. Servet-Delprat.** 2004. Immature dendritic cell transdifferentiation into osteoclasts: a novel pathway sustained by rheumatoid arthritis microenvironment. Blood **104:**4029–4037.
39. **Romas, E., M. T. Gillespie, and T. J. Martin.** 2002. Involvement of receptor activator of NFαB ligand and tumor necrosis factor-α in bone destruction in rheumatoid arthritis. Bone **30:**340–346.
40. **Santiago-Schwarz, F., P. Anand, S. Liu, and S. E. Carsons.** 2001. Dendritic cells (DCs) in rheumatoid arthritis (RA): progenitor cells and soluble factors contained in RA synovial fluid yield a subset of myeloid DCs that preferentially activate Th1 inflammatory-type responses. J. Immunol. **67:**1758–1768.
41. **Sato, K., A. Suematsu, K. Okamoto, A. Yamaguchi, Y. Morashita, Y. Kadono, S. Tanaka, T. Kodama, S. Akira, Y. Iwakura, D. J. Cua, and H. Takayanagi.** 2006. Th17 functions as an osteoclastogenic helper T cell subset that links T cell activation and bone destruction. J. Exp. Med. **203:**2673–2682.
42. **Seki, Y., H. Inoue, N. Nagata, K. Hayashi, S. Fukuyama, K. Matsumoto, O. Komine, S. Hamano, S. K. Himeno, K. Inagaki-Ohara, N. Cacalano, A. O'Garra, T. Oshida, H. Saito, J. A. Johnston, A. Yoshimura, and M. Kubo.** 2003. SOCS-3 regulates onset and maintenance of T_H2-mediated allergic responses. Nat. Med. **9:**1047–1054.
43. **Shouda, T., T. Yoshida, T. Hanada, T. Wakioka, M. Oishi, K. Miyoshi, S. Komiya, K.-I. Kosai, Y. Hanakawa, K. Hanshimoto, K. Nagata, and A. Yoshimura.** 2001. Induction of the cytokine signal regulator SOCS3/CIS3 as a therapeutic strategy for treating inflammatory arthritis. J. Clin. Investig. **108:**1781–1788.
44. **Simonet, W. S., D. L. Lacey, C. R. Dunstan, M. Kelley, M. S. Chang, R. Luthy, H. Q. Nguyen, S. Wooden, L. Bennett, T. Boone, C. Shimamoto, M. DeRose, R. Elliott, A. Colombero, H. L. Tan, G. Trail, J. Sullivan, E. Davy, N. Bucay, L. Renshaw-Gegg, T. M. Hughes, D. Hill, W. Pattison, P. Campbell, S. Sander, G. Van, J. Tarpley, P. Derby, R. Lee, and W. J. Boyle.** 1997. Osteoprotegerin: a novel secreted protein involved in the regulation of bone density. Cell **89:**309–319.
45. **Takayanagi, H.** 2007. Osteoimmunology: shared mechanisms and crosstalk between the immune and bone systems. Nat. Rev. Immunol. **7:**292–304.
46. **Taubman, M. A., and T. Kawai.** 2001. Involvement of T-lymphocytes in periodontal disease and in direct and indirect induction of bone resorption. Crit. Rev. Oral Biol. Med. **12:**125–135.
47. **Taubman, M. A., X. Han, K. B. LaRosa, S. Socransky, and D. J. Smith.** 2007. Periodontal bacterial DNA suppresses the immune response to mutan streptococcal glucosyltransferase. Infect. Immun. **75:**4088–4096.
48. **Teitelbaum, S. L.** 2006. Osteoclasts; culprits in inflammatory osteolysis. Arthritis Res. Ther. **8:**201–208.
49. **Teng, Y.-T. A., H. Nguyen, X. Gao, Y. Y. Kong, R. M. Gorczynski, B. Singh, R. P. Ellen, and J. M. Penninger.** 2000. Functional human T-cell immunity and osteoprotegerin ligand control alveolar bone destruction in periodontal infection. J. Clin. Investig. **106:**R59–R67.
50. **Teng, Y.-T. A., and W. Hu.** 2003. Expression cloning of a periodontitis-associated apoptotic effector, *cagE* homologue, in *Actinobacillus actinomycetemcomitans*. Biochem. Biophys. Res. Commun. **303:**1086–1094.
51. **Teng, Y.-T. A., and X. Zhang.** 2005. Apoptotic activity and sub-cellular localization of a T4SS-associated CagE-homologue in *Actinobacillus actinomycetemcomitans*. Microb. Pathog. **38:**125–132.
52. **Teng, Y.-T. A.** 2006. Protective and destructive immunity in the periodontium. I. Innate and humoral immunity and the periodontium. J. Dent. Res. **85:**198–208.
53. **Teng, Y.-T. A.** 2006. Protective and destructive immunity in the periodontium. 2. T-cell-mediated immunity in the periodontium. J. Dent. Res. **85:**209–119.
54. **Teng, Y.-T. A., D. Mahamed, and B. Singh.** 2005. Gamma interferon positively modulates *Actinobacillus actinomycetemcomitans*-specific $RANKL^+$ $CD4^+$ Th1-cell-mediated alveolar bone destruction in vivo. Infect. Immun. **73:**3453–3461.
55. **Theill, L. E., W. J. Boyle, and J. M. Penninger.** 2002. RANK-L and RANK: T cell, bone loss and mammalian evolution. Annu. Rev. Immunol. **20:**795–823.
56. **Travagli, J., M. Letourneur., J. Bertoglio, and J. Pierre.** 2004. STAT6 and Ets-1 form a stable complex that modulates Socs-1 expression by interleukin-4 in keratinocytes. J. Biol. Chem. **279:**35183–35192.
57. **Wada, T., T. Nakashima, N. Hiroshi, and J. M. Penninger.** 2006. RANKL-RANK signaling in osteoclastogenesis and bone disease. Trends Mol. Med. **12:**17–25.
58. **Wong, B. R., R. Josien, S. Y. Lee, B. Sauter, H. L. Li, R. M. Steinman, and Y. Choi.** 1997. TRANCE (tumor necrosis factor [TNF]-related activation induced cytokine), a new TNF family member predominantly expressed in T cells, is a dendritic cell-specific survival factor. J. Exp. Med. **186:**2075–2080.
59. **Wong, P. K. K., P. J. Egan, B. A. Croker, K. O'Donnell, N. A. Sims, S. Drake, H. K. Edward, J. McManus, S. Warren, A. Alexander, A. W. Roberts, and I. P. Wicks.** 2006. SOCS-3 negatively regulates innate and adaptive immune mechanisms in acute IL-1-dependent inflammatory arthritis. J. Clin. Investig. **116:**1571–1581.
60. **Wormald, S., J. G. Zhang, D. L. Krebs, L. A. Mielke, J. Silver, W. S. Alexander, T. P. Speed, N. A. Nicola, and D. J. Hilton.** 2006. The comparative roles of supporessor of cytokine siganling-1 and -3 in the inhibition and desensitization of cytokine signaling. J. Biol. Chem. **281:**11135–11143.
61. **Yoshimura, A., H. Nishinakamura, Y. Matsumura, and T. Hanada.** 2005. 2005. Negative regulation of cytokine signalling and immune responses by SOCS proteins. Arthrits Res. Ther. **7:**100–110.
62. **Zhang, L., D. B. Badgwell, J. J. Bevers III, K. Schlessinger, P. J. Murray, D. E. Levy, and S. S. Watowich.** 2006. IL-6 signaling via the STAT3/SOCS3 pathway: functional analysis of the conserved STAT3 N-domain. Mol. Cell. Biochem. **288:**179–189.
63. **Zhang, X., and Y.-T. A. Teng.** 2006. Interleukin-10 inhibits gram-negative-microbe specific human receptor activator of NF-κB ligand-positive $CD4^+$ Th1-cell-associated alveolar bone loss in vivo. Infect. Immun. **74:**4927–4931.

Editor: F. C. Fang